Electronic Supplementary Material (ESI) for Energy & Environmental Science.

A more stable lithium anode by mechanical constriction for solid state batteries

Yibo Su[1†], Luhan Ye[1†], William Fitzhugh[1], Yichao Wang[1], Eva Ganzales Gil[1], In Kim[1], Xin Li[1]*

[1]John A. Paulson School of Engineering and Applied Sciences, Harvard University,

Cambridge, MA 02138, USA

† Equal Contribution

* Corresponding author: lixin@seas.harvard.edu

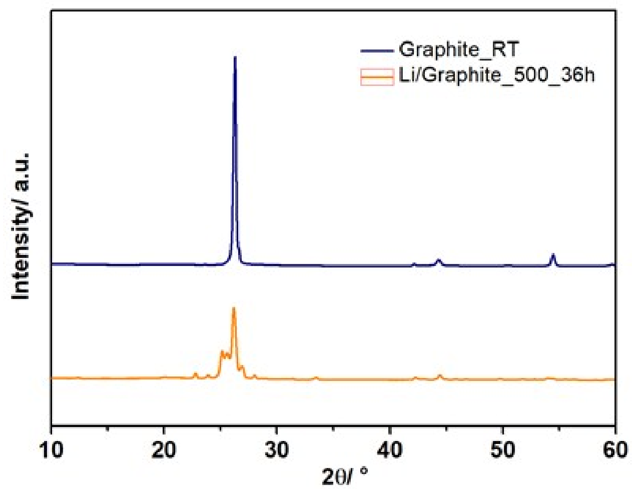

Figure S1. XRDs of graphite and the mixture of Li and graphite after heating under 500 ℃ for 36 h

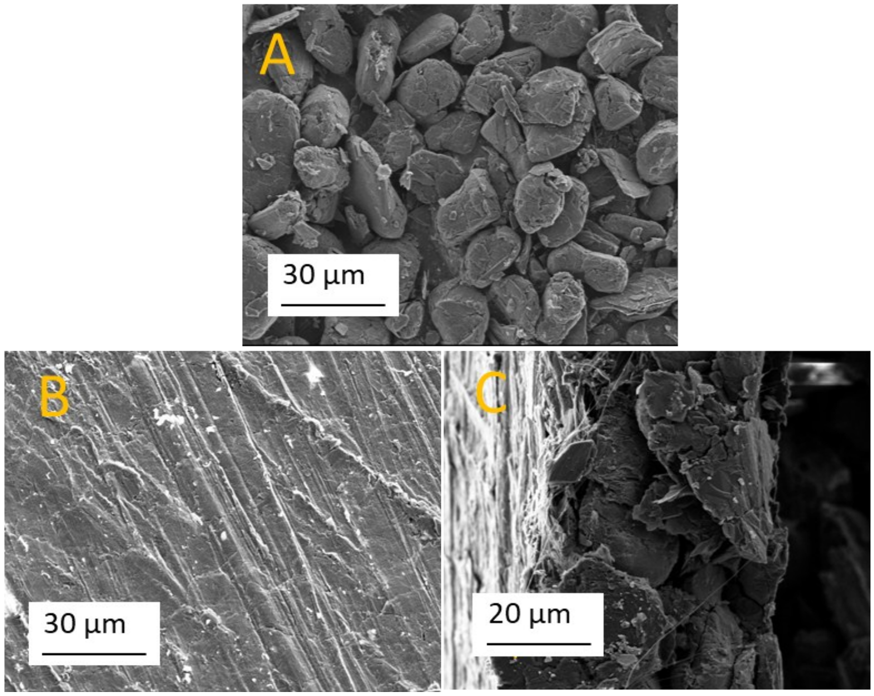

Figure S2. SEM images of (A) graphite particles; the surface (B) and cross section (C) of graphite film after pre-pressure.

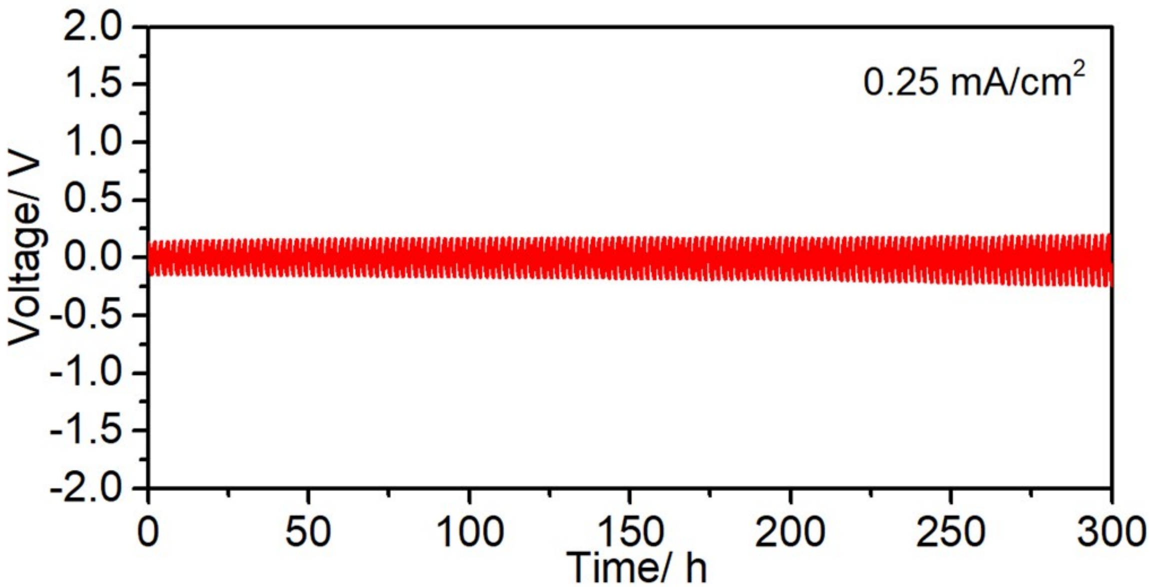

Figure S3. Cyclic performance of Li/G-LGPS-G/Li symmetric battery with relatively smaller overpotential.

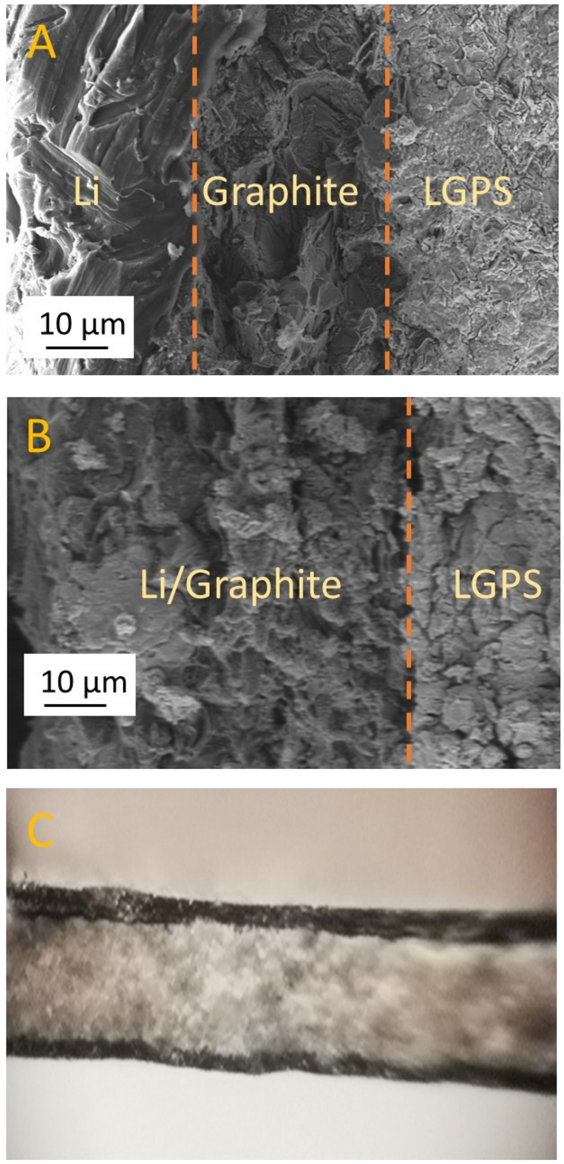

Figure S4. Comparison of SEM images of Li/G anode before (A) and after (B) long-term cycling in Fig. 2(A). (C) Optical image of Li/G-LGPS-G/Li after 300h cycling. The thickness of the pellet is around 600 µm. The color of graphite layer is black, indicating there is no obvious lithium staging in graphite in the Li/G composite during the battery cycling.

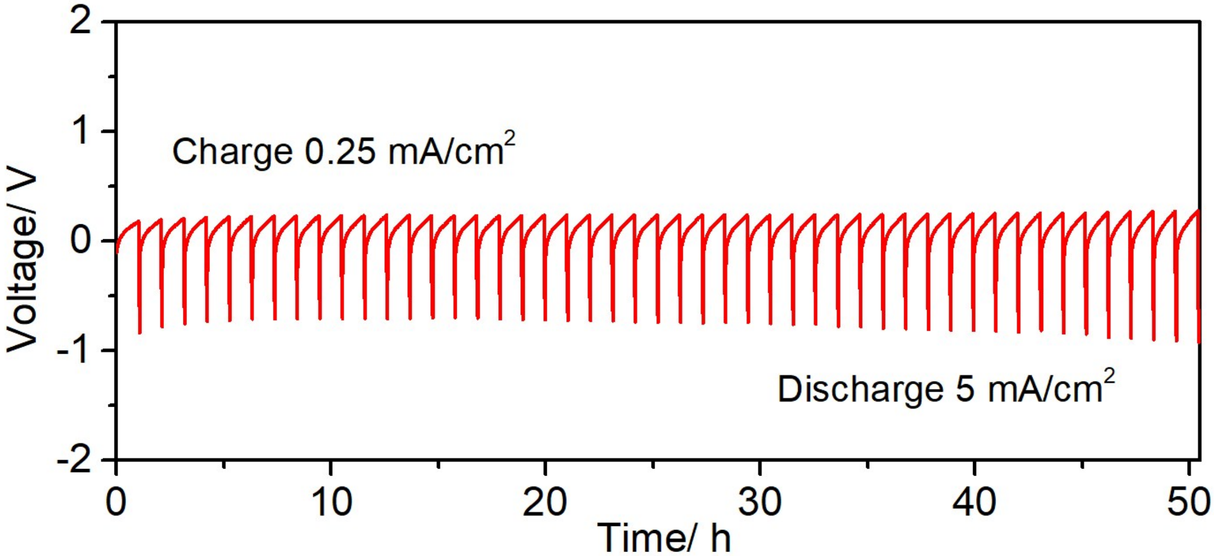

Figure S5. High rate test of Li/G-LGPS-G/Li symmetric battery. The battery is charged at 0.25mA cm^{-2} and discharge at 5mA cm^{-2}.

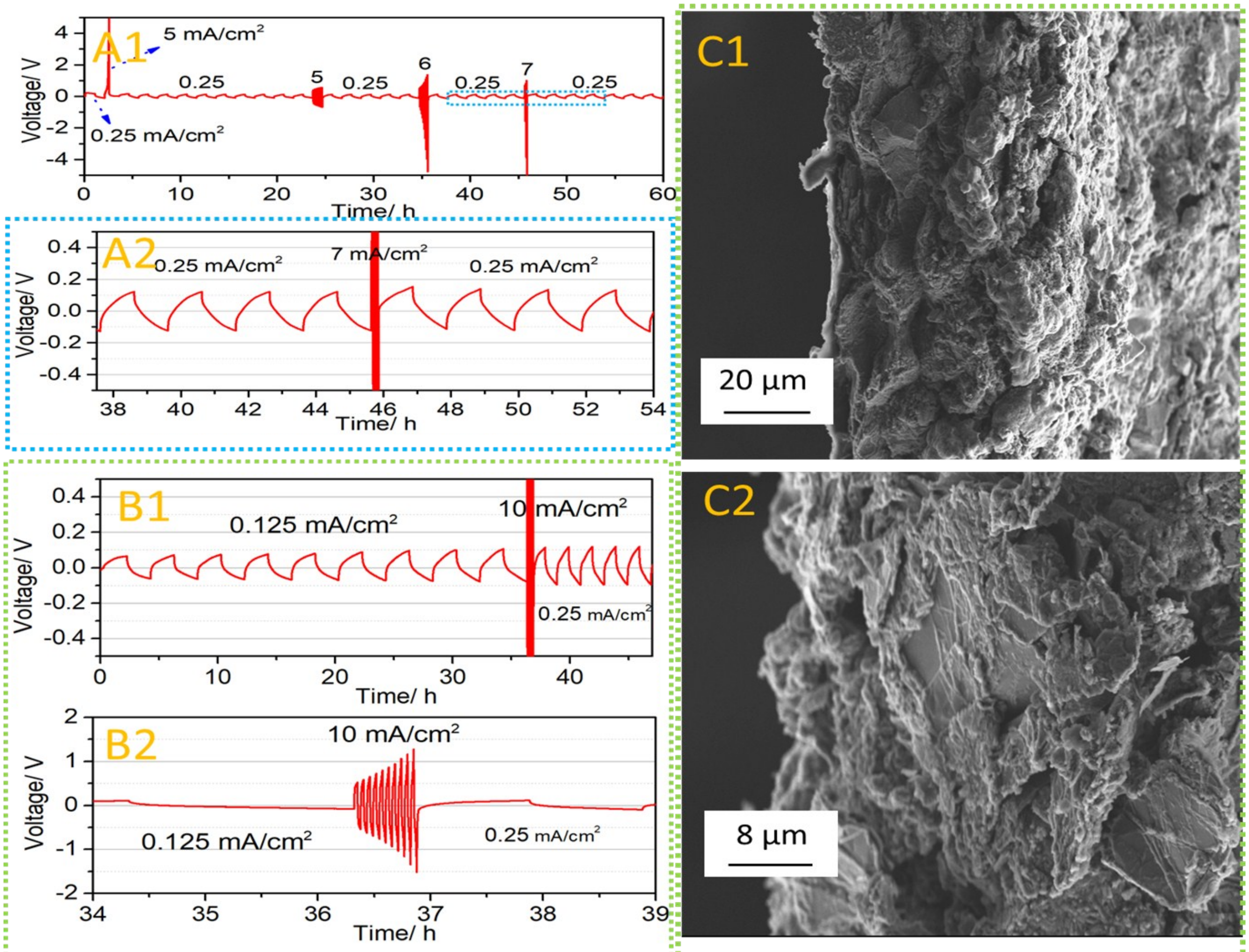

Figure S6. (A) Rate test of Li/G-LGPS-G/Li symmetric battery. When the pre-cycling time is reduced to 5 cycles at 0.25 mA cm^{-2}, the battery "fails" at 6 mA cm^{-2} or 7 mA cm^{-2}, however, when the current density is set back to 0.25 mA cm^{-2}, it always comes back normal without significant overpotential increase. (B) Enlarged Fig. 2(E2), battery cycled at 10 mA cm^{-2} plotted in a smaller voltage scale (B1) or time scale (B2). (C) SEM images of Li/Graphite composite after testing showing in B with different area and magnification. No lithium dendrite was observed. A clear 3D structure showing in Fig S6(C2).

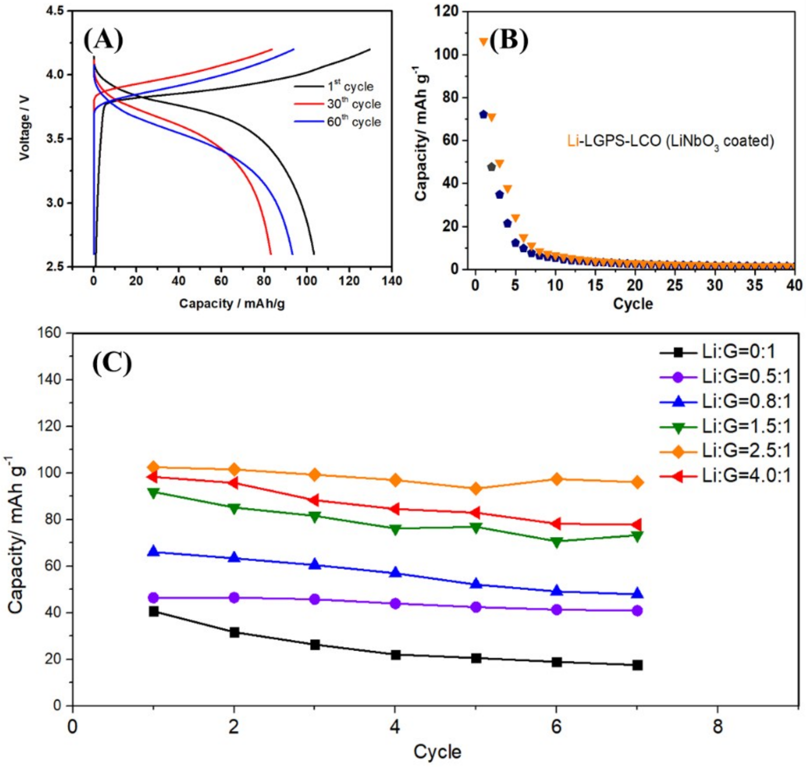

Figure S7. (A) cycling profiles of LCO-LGPS-Li/G batteries in Figure 3D. (B) Cyclic performance based on Li anode. Both batteries were tested at current density of 0.1 C at 25 ℃. (C) Cycling performance of LCO-LGPS-Li/G batteries with different Li/G ratios.

Table S1. (A)-(D) LGPS decomposition products with fraction numbers down to low voltages at different K_{eff}

(A) K_{eff} = 0 GPa

	LGPS + xLi (Reactants)	Decomposition products
2.20V	LGPS + 0.000Li	1.000 Li_4GeS_4 + 2.000 Li_3PS_4
1.73V	LGPS + 0.000Li	1.000 Li_4GeS_4 + 2.000 Li_3PS_4
1.72V	LGPS + 10.000Li	2.000 P + 8.000 Li_2S + 1.000 Li_4GeS_4
1.63V	LGPS + 10.000Li	2.000 P + 8.000 Li_2S + 1.000 Li_4GeS_4
1.62V	LGPS + 14.000Li	1.000 Ge + 2.000 P + 12.000 Li_2S
1.27V	LGPS + 14.000Li	1.000 Ge + 2.000 P + 12.000 Li_2S
1.26V	LGPS + 14.286Li	1.000 Ge + 0.286 LiP_7 + 12.000 Li_2S
1.17V	LGPS + 14.286Li	1.000 Ge + 0.286 LiP_7 + 12.000 Li_2S
1.16V	LGPS + 14.858Li	1.000 Ge + 0.286 Li_3P_7 + 12.000 Li_2S
0.94V	LGPS + 14.858Li	1.000 Ge + 0.286 Li_3P_7 + 12.000 Li_2S
0.93V	LGPS + 16.000Li	1.000 Ge + 2.000 LiP + 12.000 Li_2S
0.88V	LGPS + 16.000Li	1.000 Ge + 2.000 LiP + 12.000 Li_2S
0.87V	LGPS + 20.000Li	1.000 Ge + 2.000 Li_3P + 12.000 Li_2S
0.57V	LGPS + 20.000Li	1.000 Ge + 2.000 Li_3P + 12.000 Li_2S
0.56V	LGPS + 21.000Li	1.000 LiGe + 2.000 Li_3P + 12.000 Li_2S
0.46V	LGPS + 21.000Li	1.000 LiGe + 2.000 Li_3P + 12.000 Li_2S
0.45V	LGPS + 22.250Li	0.250 Li_9Ge_4 + 2.000 Li_3P + 12.000 Li_2S
0.29V	LGPS + 22.250Li	0.250 Li_9Ge_4 + 2.000 Li_3P + 12.000 Li_2S
0.28V	LGPS + 23.750Li	0.250 Li15Ge_4 + 2.000 Li_3P + 12.000 Li_2S
0.00V	LGPS + 23.750Li	0.250 Li15Ge_4 + 2.000 Li_3P + 12.000 Li_2S

(B) K_{eff} = 5 GPa

	LGPS + xLi (Reactants)	Decomposition products
2.20V	LGPS + 0.000Li	1.000 Li_4GeS_4 + 2.000 Li_3PS_4
1.44V	LGPS + 0.000Li	1.000 Li_4GeS_4 + 2.000 Li_3PS_4
1.43V	LGPS + 0.000Li	0.606 Li_2S + 0.038 GeP_3 + 0.962 Li_4GeS_4 + 1.886 Li_3PS_4
1.40V	LGPS + 0.000Li	3.747 Li_2S + 0.234 GeP_3 + 0.766 Li_4GeS_4 + 1.297 Li_3PS_4
1.39V	LGPS + 7.106Li	6.734 Li_2S + 0.364 GeP_3 + 0.636 Li_4GeS_4 + 0.907 Li_2PS_3
1.31V	LGPS + 12.170Li	10.261 Li_2S + 0.635 GeP_3 + 0.365 Li_4GeS_4 + 0.094 Li_2PS_3
1.30V	LGPS + 12.666Li	10.667 Li_2S + 0.667 GeP_3 + 0.333 Li_4GeS_4
1.21V	LGPS + 12.666Li	10.667 Li_2S + 0.667 GeP_3 + 0.333 Li_4GeS_4
1.20V	LGPS + 12.860Li	10.958 Li_2S + 0.667 GeP_3 + 0.097 GeS + 0.236 Li_4GeS_4
1.20V	LGPS + 12.860Li	10.958 Li_2S + 0.667 GeP_3 + 0.097 GeS + 0.236 Li_4GeS_4
1.19V	LGPS + 13.334Li	11.667 Li_2S + 0.667 GeP_3 + 0.333 GeS
1.15V	LGPS + 13.334Li	11.667 Li_2S + 0.667 GeP_3 + 0.333 GeS
1.14V	LGPS + 13.382Li	0.025 Ge + 11.691 Li_2S + 0.667 GeP_3 + 0.309 GeS

1.13V	LGPS + 13.824Li	0.246 Ge + 11.912 Li_2S + 0.667 GeP_3 + 0.088 GeS
1.12V	LGPS + 14.000Li	0.333 Ge + 12.000 Li_2S + 0.667 GeP_3
0.39V	LGPS + 14.000Li	0.333 Ge + 12.000 Li_2S + 0.667 GeP_3
0.38V	LGPS + 14.291Li	0.430 Ge + 0.291 LiP + 12.000 Li_2S + 0.570 GeP_3
0.34V	LGPS + 15.726Li	0.909 Ge + 1.726 LiP + 12.000 Li_2S + 0.091 GeP_3
0.33V	LGPS + 16.000Li	1.000 Ge + 2.000 LiP + 12.000 Li_2S
0.18V	LGPS + 16.000Li	1.000 Ge + 2.000 LiP + 12.000 Li_2S
0.17V	LGPS + 16.254Li	1.000 Ge + 1.873 LiP + 0.127 Li_3P + 12.000 Li_2S
0.09V	LGPS + 19.628Li	1.000 Ge + 0.186 LiP + 1.814 Li_3P + 12.000 Li_2S
0.08V	LGPS + 20.000Li	1.000 Ge + 2.000 Li_3P + 12.000 Li_2S
0.00V	LGPS + 20.000Li	1.000 Ge + 2.000 Li_3P + 12.000 Li_2S

(C) K_{eff} = 10 GPa

	LGPS + xLi (Reactants)	Decomposition products
2.20V	Stable	1.000 $Li_{10}Ge(PS_6)_2$
1.59V	Stable	1.000 $Li_{10}Ge(PS_6)_2$
1.54V	LGPS + 0.529Li	1.000 Li_4GeS_4 + 1.204 Li_3PS_4 + 0.531 Li_2PS_3 + 0.265 Li_7PS_6
1.51V	LGPS + 0.529Li	1.000 Li_4GeS_4 + 1.204 Li_3PS_4 + 0.531 Li_2PS_3 + 0.265 Li_7PS_6
1.50V	LGPS + 0.717Li	0.717 Li_2S + 1.000 Li_4GeS_4 + 1.283 Li_3PS_4 + 0.717 Li_2PS_3
1.40V	LGPS + 0.717Li	0.717 Li_2S + 1.000 Li_4GeS_4 + 1.283 Li_3PS_4 + 0.717 Li_2PS_3
1.39V	LGPS + 3.474Li	3.197 Li_2S + 0.092 GeP_3 + 0.908 Li_4GeS_4 + 1.724 Li_2PS_3
1.09V	LGPS + 3.560Li	3.266 Li_2S + 0.097 GeP_3 + 0.903 Li_4GeS_4 + 1.708 Li_2PS_3
1.08V	LGPS + 4.696Li	5.497 Li_2S + 0.050 GeP_3 + 0.950 GeS + 1.851 Li_2PS_3
0.72V	LGPS + 13.296Li	11.640 Li_2S + 0.664 GeP_3 + 0.336 GeS + 0.008 Li_2PS_3
0.71V	LGPS + 13.334Li	11.667 Li_2S + 0.667 GeP_3 + 0.333 GeS
0.68V	LGPS + 13.334Li	11.667 Li_2S + 0.667 GeP_3 + 0.333 GeS
0.67V	LGPS + 13.498Li	11.749 Li_2S + 0.502 GeP_3 + 0.248 GeP_2 + 0.251 GeS
0.67V	LGPS + 13.498Li	11.749 Li_2S + 0.502 GeP_3 + 0.248 GeP_2 + 0.251 GeS
0.66V	LGPS + 14.000Li	12.000 Li_2S + 1.000 GeP_2
0.00V	LGPS + 14.000Li	12.000 Li_2S + 1.000 GeP_2

(D) K_{eff} = 15 GPa

	LGPS + xLi (Reactants)	Decomposition products
2.20V	Stable	1.000 $Li_{10}Ge(PS_6)_2$
1.56V	Stable	1.000 $Li_{10}Ge(PS_6)_2$
1.54V	LGPS + 0.529Li	1.000 Li_4GeS_4 + 1.204 Li_3PS_4 + 0.531 Li_2PS_3 + 0.265 Li_7PS_6
1.51V	LGPS + 0.529Li	1.000 Li_4GeS_4 + 1.204 Li_3PS_4 + 0.531 Li_2PS_3 + 0.265 Li_7PS_6
1.50V	LGPS + 0.717Li	0.717 Li_2S + 1.000 Li_4GeS_4 + 1.283 Li_3PS_4 + 0.717 Li_2PS_3
1.40V	LGPS + 0.717Li	0.717 Li_2S + 1.000 Li_4GeS_4 + 1.283 Li_3PS_4 + 0.717 Li_2PS_3
1.39V	LGPS + 3.474Li	3.197 Li_2S + 0.092 GeP_3 + 0.908 Li_4GeS_4 + 1.724 Li_2PS_3
1.09V	LGPS + 3.474Li	3.197 Li_2S + 0.092 GeP_3 + 0.908 Li_4GeS_4 + 1.724 Li_2PS_3
1.08V	LGPS + 4.368Li	5.263 Li_2S + 0.026 GeP_3 + 0.974 GeS + 1.921 Li_2PS_3
0.58V	LGPS + 6.148Li	6.535 Li_2S + 0.154 GeP_3 + 0.846 GeS + 1.539 Li_2PS_3

0.57V	LGPS + 6.362Li	6.653 Li_2S + 0.236 GeP_2 + 0.764 GeS + 1.528 Li_2PS_3
0.43V	LGPS + 8.690Li	8.283 Li_2S + 0.469 GeP_2 + 0.531 GeS + 1.062 Li_2PS_3
0.42V	LGPS + 9.166Li	9.306 Li_2S + 1.000 GeS + 0.861 P_2S + 0.277 Li_2PS_3
0.38V	LGPS + 9.918Li	9.932 Li_2S + 1.000 GeS + 0.986 P_2S + 0.027 Li_2PS_3
0.37V	LGPS + 10.000Li	10.000 Li_2S + 1.000 GeS + 1.000 P_2S
0.37V	LGPS + 10.000Li	10.000 Li_2S + 1.000 GeS + 1.000 P_2S
0.36V	LGPS + 10.110Li	10.055 Li_2S + 0.027 GeP_2 + 0.973 GeS + 0.973 P_2S
0.09V	LGPS + 13.900Li	11.950 Li_2S + 0.975 GeP_2 + 0.025 GeS + 0.025 P_2S
0.08V	LGPS + 14.000Li	12.000 Li_2S + 1.000 GeP_2
0.00V	LGPS + 14.000Li	12.000 Li_2S + 1.000 GeP_2

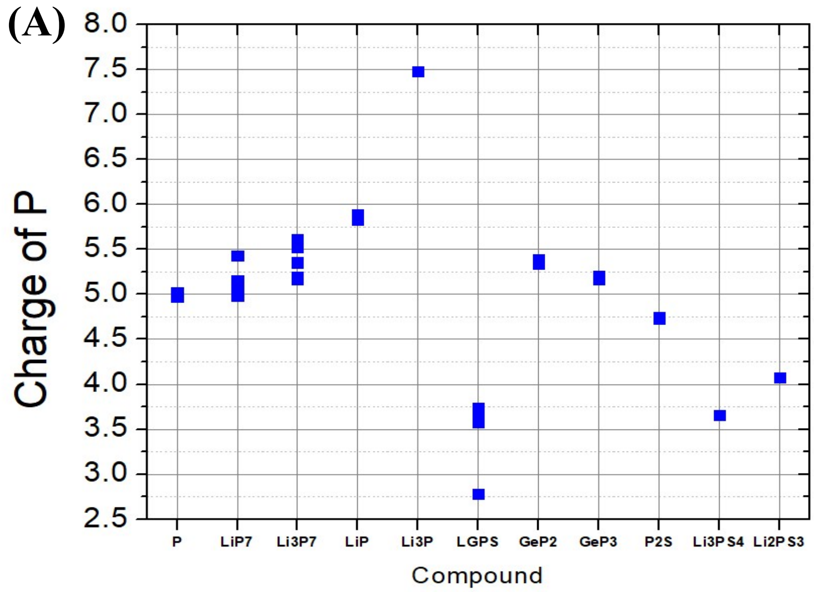

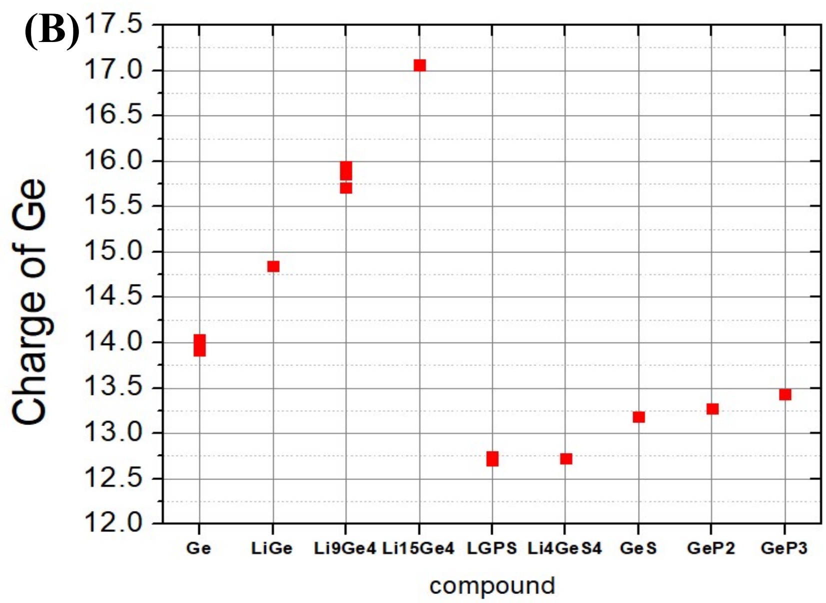

Figure S8. Bader charge analysis from DFT simulations. (A) Phosphorus element in all the P-related compounds from the decomposition product list; (B) Ge element in all the Ge-related compounds from the decomposition product list.

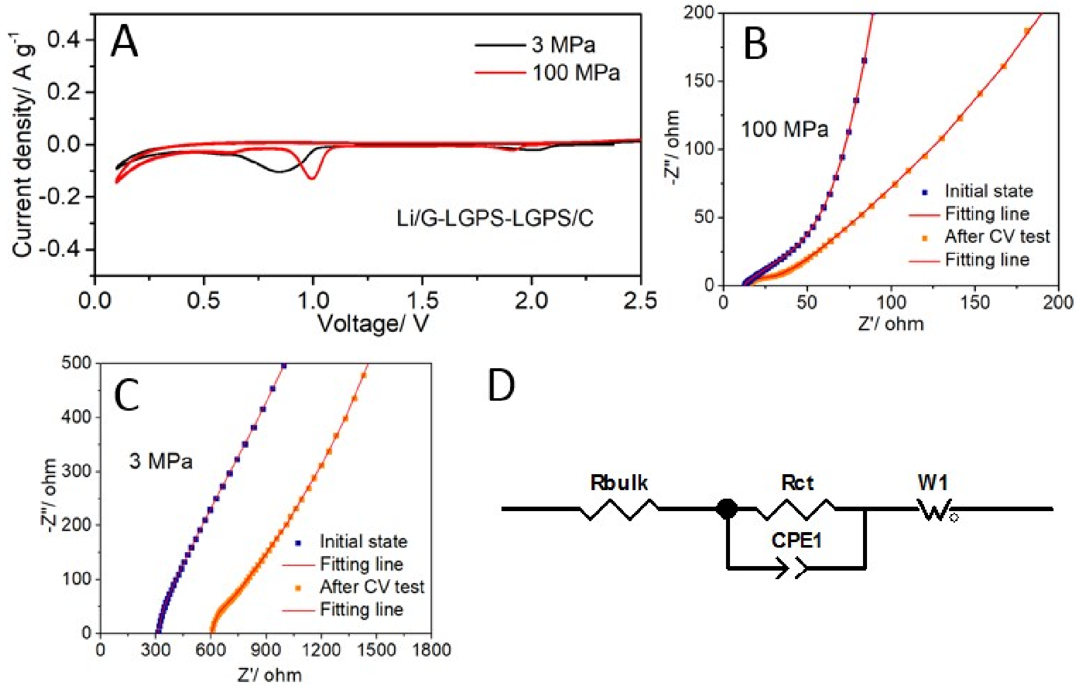

Figure S9. (A) Comparison of CV curves of Li/G-LGPS-LGPS/C battery tested under 3 and 100 MPa; (B,C) comparison of impedance change before and after these two CV tests; (D) Model used in impedance fitting. R_{bulk} stands for the ionic diffusion resistance and R_{ct} represents the charge transfer resistance. All EIS data are fitted with Z-view.

Table S2. Calculated R_{bulk} and R_{ct}

	R_{BULK} /Ω	**R_{CT} /Ω**	**R_T /Ω**
100 MPa-Initial	13.4	38.8	52.2
100 MPa -CV	13.7	20.7	34.4
3 MPa -Initial	313.7	395.4	709.1
3 MPa -CV	606.0	285.3	891.3

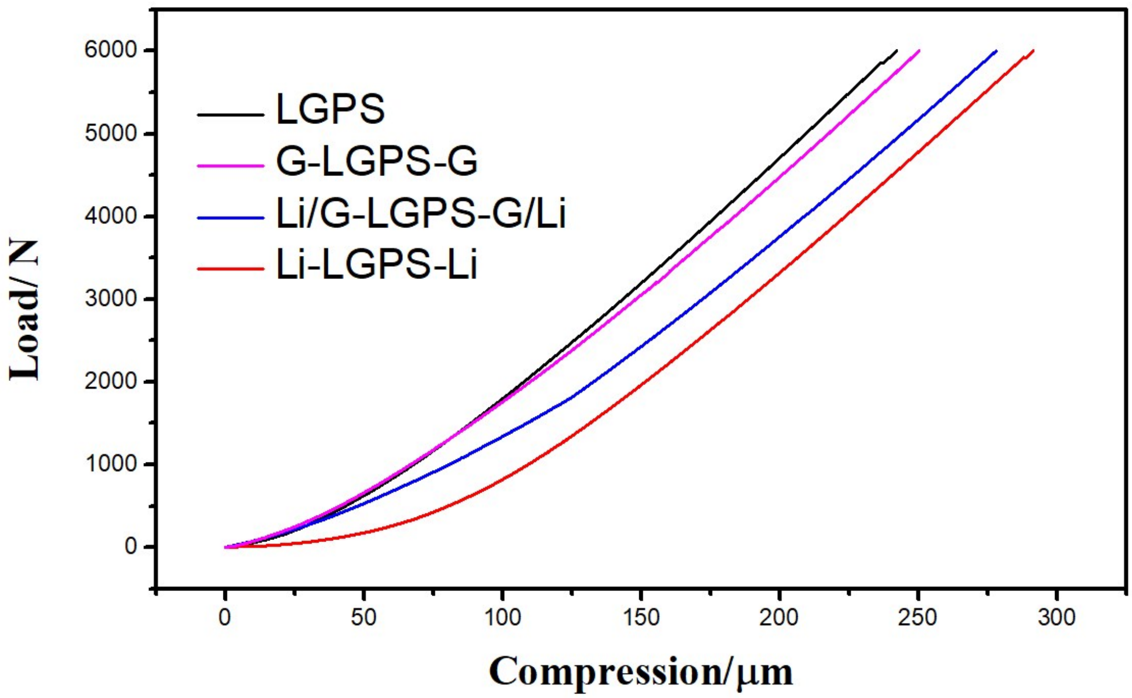

Figure S10. The thickness change of LGPS, G-LGPS-G, Li-LGPS-Li, and Li/G-LGPS-G/Li pellets under pressure. The pellets were pre-pressed to the initial thicknesses of 474 µm, 502 µm, 549 µm and 577 µm, respectively. The diameter of the pellet is ½ inch.